Chapter 7
The Fatigue Strength of Notched Specimens

Frequently used symbols

S	nominal stress
σ	local stress
S_{f1}	fatigue limit of unnotched specimens
S_{fk}	fatigue limit of notched specimens
K_t	stress concentration factor
K_f	fatigue strength reduction factor
ρ	tip radius of notch
a^*, A	material constants depending on S_U
S_U	tensile strength

7.1 Introduction

Material fatigue properties obtained on unnotched specimens were discussed in the previous chapter. However, an engineering structure is not an unnotched specimen. On the contrary, various "notched" elements can

always be indicated in a structure. Fatigue tests on notched specimens are necessary for two major purposes:

(1) To arrive at prediction methods for fatigue properties of structural elements.
(2) To carry out comparative fatigue tests to explore effects of different variables.

The first topic is covered in the present chapter, while the second topic is addressed in Chapter 13.

Engineering fatigue properties to be predicted are primarily associated with the fatigue limit and S-N curves. Predictions of the fatigue limit of a notched element is a more well defined problem than predictions of S-N curves. With respect to the fatigue limit, it is a matter of predicting whether a crack will be nucleated at the root of a notch, or whether that will not occur. For several engineering applications that is indeed a design criterion. It boils down to a prediction of a threshold stress level. However, for S-N curves, i.e. finite fatigue lives, the prediction problem is fundamentally different because the fatigue life to be predicted covers a crack initiation life and a crack growth life. Usually, the crack growth life for many structural elements, and also for fatigue specimens, is relatively short. It covers a small percentage of the total fatigue life. This aspect is generally disregarded in engineering prediction methods. As a consequence, it affects accuracies of prediction methods. It implies that predictions then give indications which should be handled with care, actually with engineering judgement.

In this chapter, fatigue properties of notched specimens are addressed first. The specimens are supposed to be representative for simple notches occurring in a real structure; notches with a well defined geometry for which the stress concentration factor (K_t) is available or can be calculated (e.g. holes, fillets, rounded corners, etc.). It starts with predictions of the fatigue limit based on the similarity of stress cycles in notched and unnotched specimens. Several variables are considered, the effect of a mean stress, different types of loading, and the effect of the quality of the material surface (surface finish). This is mainly restricted to effects on the fatigue limit. It is illustrated with some examples of predicting the fatigue limit of structural elements. Finally the prediction of S-N curve is addressed.

The present chapter is restricted to fatigue under constant-amplitude loading. Fatigue notch problems under variable-amplitude loading are discussed in Chapter 10. More complex notches occurring in various types of joints are covered in later chapters (Chapters 18 and 19). Fatigue of full-scale structures including additional variables and design problems are discussed

in Chapter 20. The major points of the present chapter are summarized in the last section of this chapter.

7.2 The fatigue limit of notched specimens at $S_m = 0$

7.2.1 The similarity principle and the notch sensitivity

After fatigue was recognized in the previous century as a serious threat to the integrity of a structure, it was soon understood that stress concentrations aggravate the fatigue problem considerably. Many early fatigue experiments on the effect of notches on fatigue were carried out on small rotating beam specimens with circumferential notches with rather sharp root radii. This is remarkable because fatigue occurred in rather massive structures. Several early test programs were carried out on specimens with diameters of about 10 mm, a notch depth in the order of 1 to 2 mm, and notch root radii as small as 0.1 mm. Notches with such small root radii are now considered to be a poor fatigue design case, and not a realistic simulation of notches in a well designed structure. In the 1930s [1], it was already known from experiments that larger specimens with larger root radii, but the same K_t, could have a lower fatigue limit. In other words; a size effect on the fatigue limit of notched elements was discovered.

In order to understand and to predict the notch effect and the size effect on the fatigue limit, the definition of the fatigue limit must be recalled. It is the lowest stress amplitude which is still capable to nucleate a microcrack that can grow to failure, or, similarly the highest stress amplitude just not capable to create such a microcrack. Keeping this definition in mind, the similarity principle can be applied to compare fatigue in a notched specimen to fatigue in an unnotched specimen, see Figure 7.1. If a cycle with a stress amplitude S_a can create a microcrack in the unnotched specimen, the same cycle of the peak stress in the notched specimen, σ_{peak}, should also be capable to create a microcrack at the root of the notch. If S_a in the unnotched specimen is the fatigue limit (S_{f1}) of that specimen, then S_{peak} in the notched specimen should correspond to the fatigue limit of the notched specimen (S_{fk}). The similarity principle thus leads to:

$$S_{\text{peak}} = K_t S_{fk} = S_{f1} \quad \text{or} \quad S_{fk} = \frac{S_{f1}}{K_t} \tag{7.1}$$

It implies that the fatigue limit of an unnotched specimen should be divided by K_t to obtain the fatigue limit of the notched specimen. However, it has

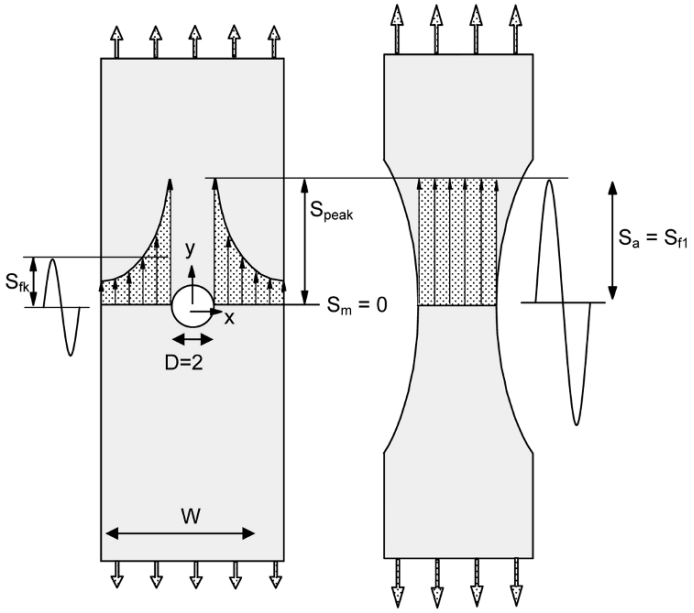

Fig. 7.1 Similarity principle: same S_{peak} at fatigue limit.

been shown in numerous fatigue tests that the reduction factor is smaller than K_t. The reduction factor obtained by experiments is denoted by the symbol K_f. It implies that

$$S_{fk} = \frac{S_{f1}}{K_f} \quad \text{or} K_f = \frac{S_{f1}}{S_{fk}} \tag{7.2}$$

K_f is also labeled as the fatigue notch factor. Experimental evidence thus indicated that

$$K_f \leq K_t \tag{7.3}$$

Long ago it was often observed that $K_f < K_t$, especially for small specimens with high K_t-values, and the more so for low-strength materials, such as low-carbon steel. Although $K_f < K_t$ apparently limits the applicability of the similarity principle, it should be noted that the inequality is favorable. If K_f is smaller than K_t, it implies that a material is less notch sensitive than predicted by $K_f = K_t$. The notch sensitivity of a material as considered by Peterson [1] was defined by a factor q as

$$q = \frac{K_f - 1}{K_t - 1} \tag{7.4}$$

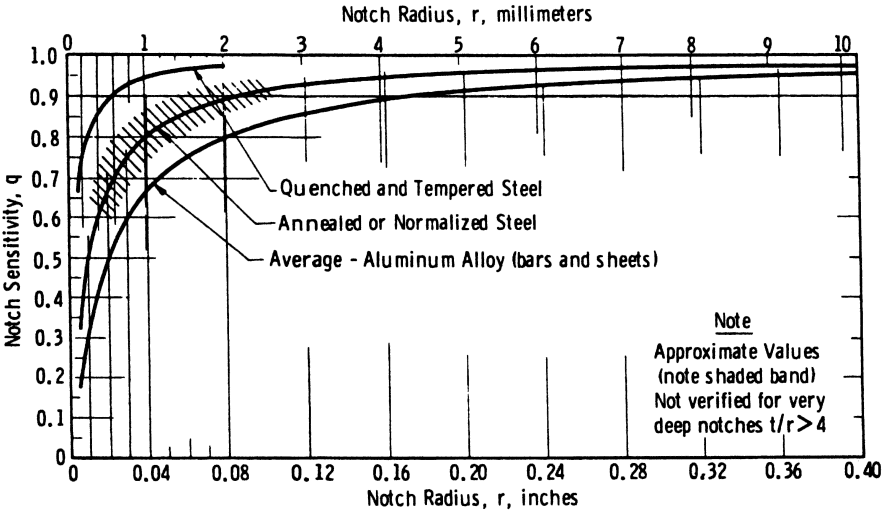

Fig. 7.2 The notch sensitivity of the fatigue limit ($S_m = 0$) of rotating beam specimens. Average results for different sizes (root notch) and material strength [1].

A high notch sensitivity is obtained if $K_f = K_t$ and thus $q = 1$. If there is no notch sensitivity, then $K_f = 1$ and thus $q = 0$. A variation of q from 0 to 1 corresponds to an increasing notch sensitivity. The factor q was used by Peterson [1] to illustrate both effects of the material strength and the size of specimens. A graph of Peterson is shown in Figure 7.2 with q-values between 0 and 1. It shows that q is larger for stronger materials and for larger specimens. In order to explain these trends the similarity principle as applied in Figure 7.1 must be reconsidered.

7.2.2 The size effect on the fatigue limit of notched specimens

Comments on size effects were already made in the discussions on Figures 3.7 to 3.9. It was pointed out that a size effect could depend on the amount of material with a high cyclic stress. For a notched specimen, it depends on stress gradients at the root of the notch. It was concluded in Section 3.3 that the variation of the stress along the material surface is very important because crack nucleation is a material surface phenomenon. This aspect was also considered in Chapter 6 (Section 6.3.3) in the discussion of a size effect on the fatigue limit of unnotched specimens. It was said that nominally unnotched specimens are always slightly notched. In spite of

that, the area of highly stressed surface material of an unnotched specimen is generally larger than for a notched specimen. The straight forward similarity approach leading to $K_f = K_t$ does not give credit to the non-similarity of the highly stressed surface area of notched and unnotched specimens. As a consequence, a size effect can occur leading to a higher fatigue limit of a notched specimen than expected from $K_f = K_t$, and thus to $K_f < K_t$.

It is an intriguing but difficult question how the size effect on the fatigue limit of notched specimens can be accounted for in a quantitative way. The effect should be related to the probability of favorable locations for microcrack nucleation at the root of a notch. The question is whether the probability should be considered to be a volume effect (3D), or a surface effect (2D), or a corner edge effect (1D). The probability of having favorable sites for microcrack initiation can also depend on the type of material including inclusions and impurities. Although the presence of a size effect can be understood in a qualitative way, it must be admitted that K_f cannot be derived from K_t in a strictly rational way. Moreover, the fatigue limit of the unnotched specimen (S_{f1}) is also depending on the specimen type and size. Under such conditions, it is not surprising that semi-empirical relations were proposed to account for the size effect. Three different approaches were proposed in the literature which are discussed below. They are associated with the names of Peterson [1], Neuber [2] and Siebel [3].

Prediction method of Peterson

Peterson [1] considered the steep stress gradient in the direction perpendicular to the material surface, i.e. $\mathrm{d}\sigma_y/\mathrm{d}x$ at the root notch (see Section 3.3). He thought that the stress level σ_y at a small distance δ below the surface could be used as a criterion for the fatigue limit of a notched element. This stress level is approximately equal to:

$$\sigma_{\text{peak}} - \delta \left(\frac{\mathrm{d}\sigma_y}{\mathrm{d}x} \right)_{x=\rho} \tag{7.5}$$

Peterson proposed the following relation for the notch sensitivity defined in Equation (7.4):

$$q = \frac{K_f - 1}{K_t - 1} = \frac{1}{1 + a^*/\rho} \tag{7.6}$$

with ρ as the notch root radius and a^* as a material constant depending on the material. This equation cannot be derived by using Equation (7.5). But the equation agreed with average results of data on the fatigue limit

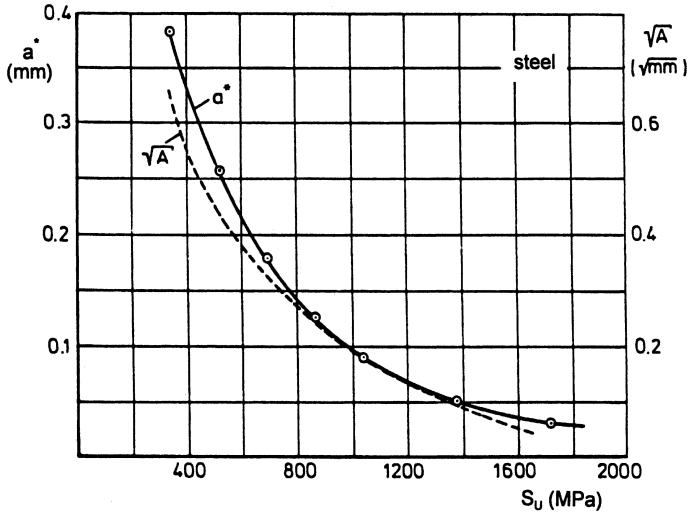

Fig. 7.3 Material constants a^* (Peterson [1]) and $\sqrt{A}$ (Kuhn and Hardrath [3]) to predict the fatigue limit ($S_m = 0$) of notched steel specimens.

for $S_m = 0$ which were available to Peterson in the 1950s. In Figure 7.2: $a^* = 0.063$ mm (0.0025 inch) for quenched and tempered steel (high strength), $a^* = 0.254$ mm (0.01 inch) for annealed or normalized steel (low strength), and $a^* = 0.51$ mm (0.02 inch) for Al-alloy sheets and bars. It is easily observed from Equation (7.6) that K_f will approach K_t for a small a^* and for a large root radius ρ. On the contrary, K_f becomes much smaller than K_t if ρ is very small (i.e. sharp notches with a small root radius). Peterson presented a^*-values for steels of different ultimate tensile strength levels. These empirically obtained values are plotted in Figure 7.3. The a^*-value is decreasing for an increasing S_U, and thus the notch sensitivity of the fatigue limit becomes more severe.

Prediction method of Neuber

Neuber is the author of a famous book on elastic stress distributions in notched elements (first edition in 1937, and translated in 1946 [2]). He noticed that the K_t-values obtained by elastic stress analysis highly overestimated the notch severity in experiments. Neuber then proposed an effective stress concentration factor, K_N, which is

$$K_N = 1 + \frac{K_t - 1}{1 + \frac{\pi}{\pi - \omega}\sqrt{A/\rho}} \tag{7.7}$$

Again ρ is the root radius, A is a material constant, and ω the opening angle of a V-notch. For $\omega = 0$ and considering that K_N is the fatigue reduction factor K_f, Equation (7.8) reduces to

$$q = \frac{K_f - 1}{K_t - 1} = \frac{1}{1 + \sqrt{A/\rho}} \tag{7.8}$$

Neuber discussed a relation between A and the average stress in a thin surface layer, but he did not give a derivation of Equation (7.8). Surprisingly enough, Neuber dropped the K_N equation in the second edition of his book (in 1958). However, Equation (7.8) was still evaluated by Kuhn and Hardrath [3] in the 1950s, and they found it to be a reasonably accurate engineering equation for different steels and Al-alloys. The value of A was considered to be a material constant which for steel varied in a way much similar to the variation of a^* of Peterson, see Figure 7.3. Kuhn and Hardrath give $A = 0.5$ mm (0.02 inch) for the Al-alloys 2024-T3 and 7075-T6.

The similarity and the difference between the equations of Peterson and Neuber are easily observed. The meaning of a^* and $\sqrt{A}$ is similar. However, the effect of ρ (size effect) appears in a different way as $1/\rho$ in the denominator of Equation (7.6), and $1/\sqrt{\rho}$ in Equation (7.8). Actually, the differences between the results obtained with the two equations are quantitatively fairly small. As an example, the ratio between the K_f-values are calculated for some different strength levels of steel with the values of a^* and $\sqrt{A}$ in Figure 7.3. Calculations for $K_t = 2.5$ and $\rho = 2.5$ mm then give the following ratios:

S_U (MPa)	400	800	1200	1600
(K_f) Neuber / (K_f) Peterson	0.91	0.95	0.97	0.99

For a low-C steel (K_f) Neuber is 9% lower than (K_f) Peterson, but for steels with a high-strength level, which are the more fatigue sensitive steels, the differences are practically negligible.

For engineering applications it is of some interest to know whether K_f is smaller than K_t, and how much smaller. This is not easily observed from Equation (7.8), but this equation can be rewritten as

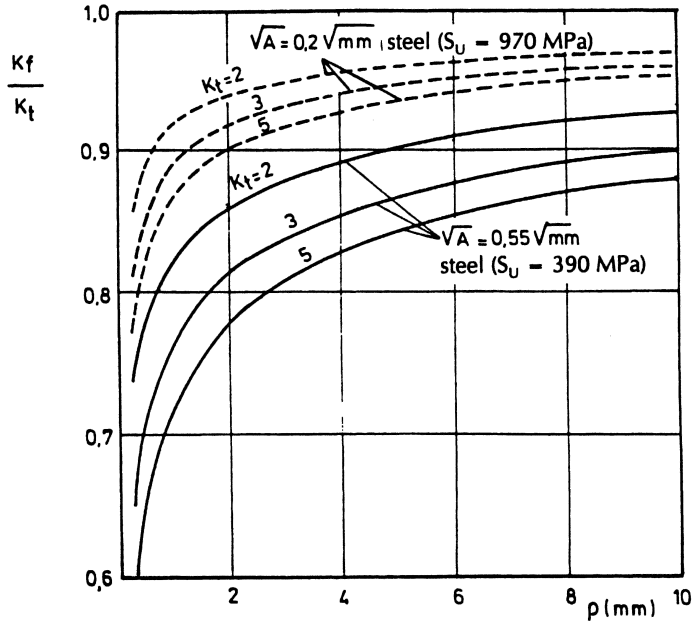

Fig. 7.4 The effects of the size (ρ), the K_t-value, and two different strength levels of steel on the ratio K_f/K_t according to the Neuber equation.

$$\frac{K_f}{K_t} = \frac{1 + \frac{1}{K_t}\sqrt{A/\rho}}{1 + \sqrt{A/\rho}} \tag{7.9}$$

This ratio has been calculated for a low-strength steel ($S_U = 390$ MPa) and a high-strength steel ($S_U = 970$ MPa). The corresponding $\sqrt{A}$-values of Figure 7.3 were used. The K_f/K_t ratio was calculated for $K_t = 2$, 3 and 5 respectively. The results in Figure 7.4 indicate that K_f is significantly smaller than K_t if the root radius is small. For larger root radii and more fatigue sensitive high-strength steel, K_f/K_t is of the order of 0.95, i.e. the difference between K_f and K_t is about 5%. In other words; assuming $K_f = K_t$ can hardly be considered to add some hidden safety margin. Only for low-strength steel some appreciable advantage exists because then K_f is substantially smaller than K_t. In other words, the material is apparently less fatigue notch sensitive.

Prediction method of Siebel

Around 1950 Siebel and coworkers [4] proposed an other approach to predict notch and size effects on the fatigue limit at $S_m = 0$. The effects are assumed to be a function of the "relative" stress gradient at the root of the notch indicated by the symbol χ:

$$\chi = \frac{\left(\frac{\mathrm{d}S_y}{\mathrm{d}x}\right)_{\text{notch root}}}{S_{\text{peak}}} \tag{7.10}$$

The stress gradient was discussed in Chapter 3. Equation (3.10) is recalled here:[12]

$$\left(\frac{\mathrm{d}S_y}{\mathrm{d}x}\right)_{\text{notch root}} = \left(2 + \frac{1}{K_t}\right)\frac{S_{\text{peak}}}{\rho} = \alpha\frac{S_{\text{peak}}}{\rho} \tag{3.10}$$

with $\alpha = 2 + 1/K_t$. Combining the two equations gives

$$\chi = \frac{\alpha}{\rho} \tag{7.11}$$

As pointed out in Chapter 3, the variation of α is fairly small for technical notches with K_t in the range 2 to 5. Siebel et al. adopted $\alpha = 2$ for tension and bending. Instead of the ratio K_f/K_t, they considered the inverse ratio $n_\chi = K_t/K_f$. This ratio was proposed to be a function of the relative stress gradient χ. The function was empirically obtained for various materials and represented by

$$n_\chi = 1 + \sqrt{s_g \chi} \tag{7.12}$$

with the material constant s_g accounting for the type of material. The equation can be rewritten with $n_\chi = K_t/K_f$, $\chi = \alpha/\rho$ and $\alpha = 2$:

$$\frac{K_f}{K_t} = \frac{1}{1 + \sqrt{s_g \chi}} = \frac{1}{1 + \sqrt{A^*/\rho}} \tag{7.13}$$

with $A^* = 2s_g$ as the material constant. A comparison of Equation (7.13) with the Neuber equation (7.9) illustrates the similarity as well as the difference between the two prediction methods. In the Siebel equation (7.13), the ratio K_f/K_t depends on the size (ρ), but not on K_t whereas in the Neuber equation (7.11) the ratio depends on both. However, in the numerator of the Neuber equation $(1/K_t)/\sqrt{A}/\rho$ is usually much smaller than 1, and thus

[12] Siebel et al. considered the absolute value of the stress gradient. The minus sign of Equation (3.10) in Chapter 3 has been dropped for that reason.

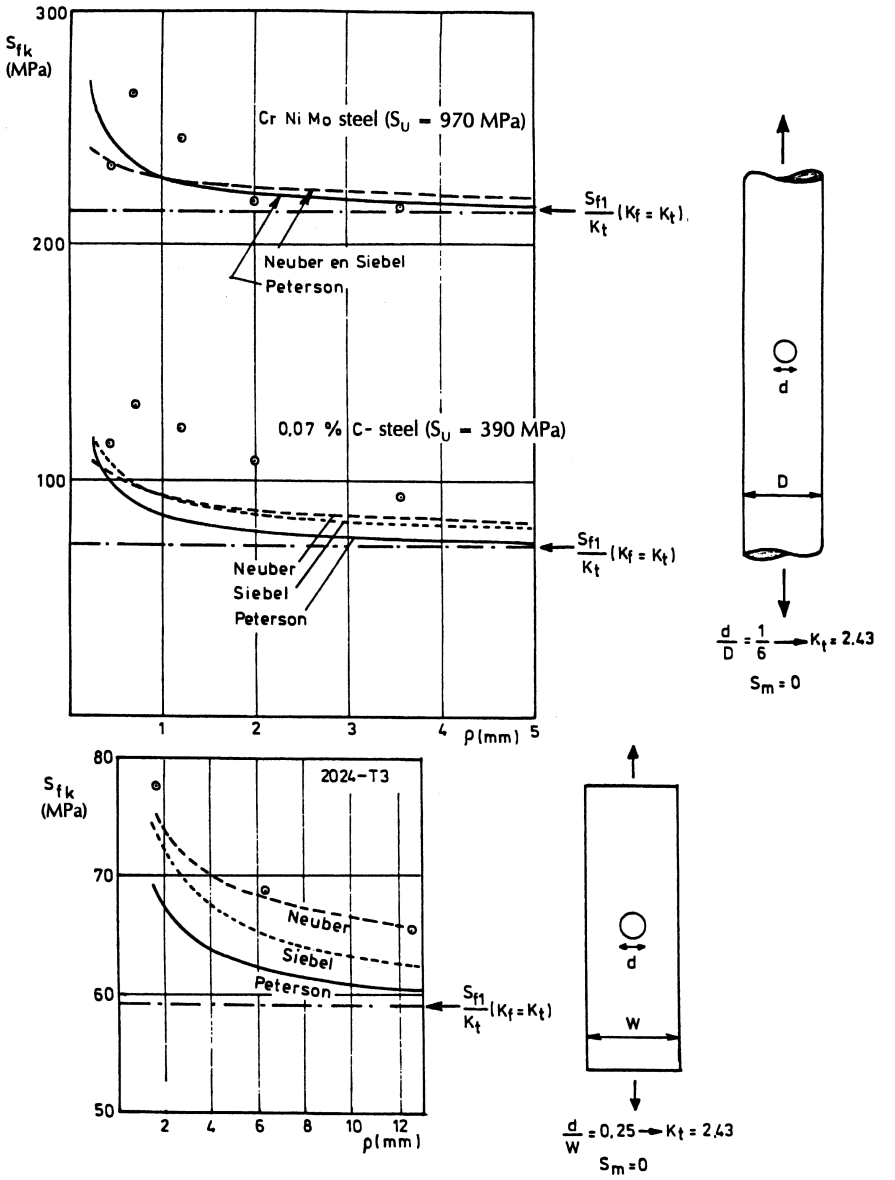

Fig. 7.5 Size effect on the fatigue limits ($S_m = 0$) of two steels [5] and an Al-alloy [6]. Comparison between three prediction methods.

both equations could still give approximately similar predictions This is illustrated in Figure 7.5 by empirical data for mild steel, a low-alloy steel and an Al-alloy. Only the size effect is checked by the results because K_t is

not a variable in this figure. Two simple specimens are involved, a round bar with a transverse hole and a flat sheet specimen with a central hole. In all three cases an increasing fatigue limit occurs for smaller holes except for the smallest hole in both steels with $\rho = 0.4$ mm. This unsystematic result could be due to the drilling operation of such a small hole. Disregarding the results of the smallest hole in steel, Figure 7.5 illustrates a systematic size effect, but it also shows that highly accurate predictions were not obtained. Secondly, the predictions for the two steels are quite similar for the three prediction methods. The differences appear to be larger for the Al-alloy, but still within 10%. The agreement of the predictions with the test results is good for the low-alloy steel for the larger two holes ($\rho = 2.0$ and 3.6 mm). For the mild steel specimens, the fatigue limit is underestimated, slightly more so by the Peterson method. The underestimation is some 10 to 20% for the other two methods. The Neuber predictions for the Al-alloy are quite good whereas the other two methods give some underestimations.

7.3 The fatigue limit of notched specimens for $S_m > 0$

Local plastic deformation at the root of a sharp notch was not considered in the previous section on the fatigue limit of a notched specimen at $S_m = 0$. It is possible that some cyclic plastic deformation occurs in notched specimens of a soft material, but at the stress amplitude of the fatigue limit this will be stopped due to cyclic strain hardening.

The situation becomes different if a positive mean stress is present ($S_m > 0$). The stress cycle is no longer symmetric around a zero mean value. Figure 7.6 gives the stress distribution in a notched specimen for the maximum and minimum load of a cycle. The peak stress at the edge of the hole varies between $K_t S_{\max}$ and $K_t S_{\min}$ provided the material response is still elastic. The stress concentration factor K_t must then be applied to both $S_{\max}$ and $S_{\min}$. It also implies that the mean stress and the stress amplitude at the root of the notch are K_t times the net section values (see Figure 7.6):

$$S_{\max,\text{peak}} = K_t S_{\max}, \quad S_{\min,\text{peak}} = K_t S_{\min}$$
$$S_{a,\text{peak}} = K_t S_a, \quad S_{m,\text{peak}} = K_t S_m \tag{7.14}$$

If the same peak stress levels occur in an unnotched specimen, the same fatigue damage response should be expected according to the similarity principle. The same fatigue limit threshold stress levels should be applicable. The prediction of the fatigue limit of notched specimens employing the

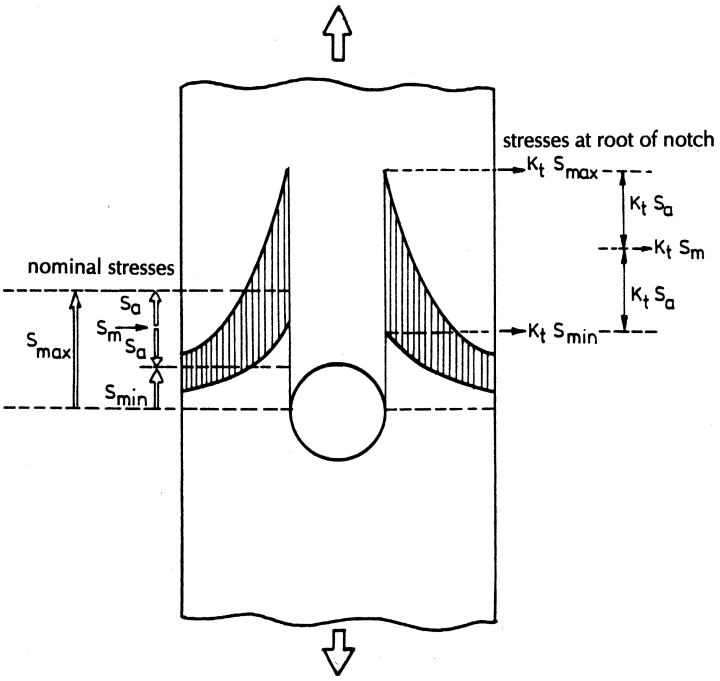

Fig. 7.6 Elastic behavior at notch root. $S_m > 0$.

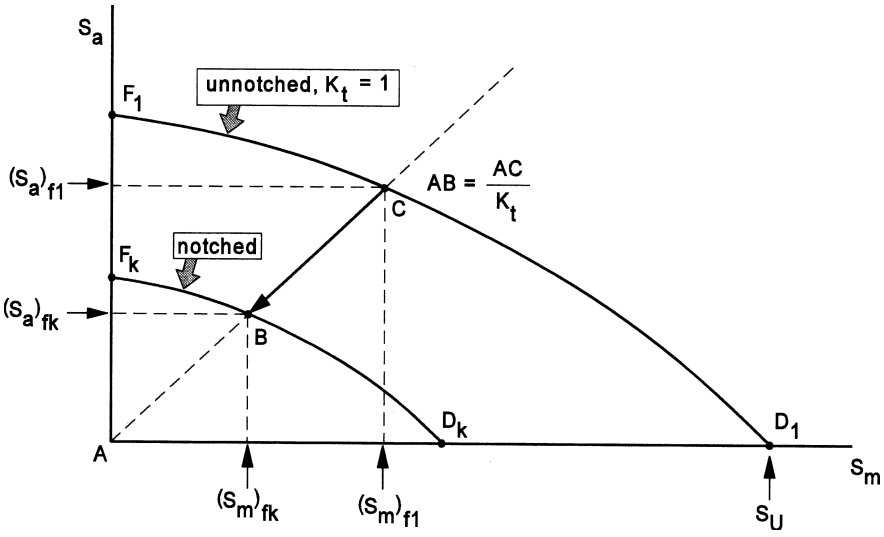

Fig. 7.7 Prediction of the fatigue limit of a notched specimen. Application of K_t to both S_a and S_m.

fatigue limit data of unnotched specimens is illustrated by Figure 7.7. The upper line in this figure gives the fatigue limit of the unnotched specimen, $S_{a,f1}$, as a function of the mean stress, $S_{m,f1}$. The subscript $f1$ refers to the fatigue limit of the unnotched specimen ($K_t = 1$), see point C in Figure 7.7. The subscript fk is used for the fatigue limit of the notched specimen. Point B on the line AC in Figure 7.7 is obtained by dividing $S_{a,f1}$ and $S_{m,f1}$ by K_t, which leads to $S_{a,fk} = S_{a,f1}/K_t$ and $S_{m,fk} = S_{m,f1}/K_t$. If C is a fatigue limit of the unnotched material, it implies that the corresponding fatigue limit of the notched specimen is obtained as point B. In this way, the entire line F_1-D_1 for the unnotched specimen is converted to the line F_k-D_k for the notched specimen.

The application of K_t to both S_m and S_a can lead to a reasonable approximation for the fatigue limit at low S_m-values. However, for a high S_m-value this cannot be true. The $S_{a,fk}$ line does not go to point D_k in Figure 7.7. In reality, the fatigue limit $S_{a,fk}$ line goes to zero (i.e. no cyclic load) at a stress level in the order of the static strength of the notched specimen. The notch effect on the static strength is rather small, at least if the material still has some ductility. In a static test on a notched specimens, significant plastic deformation occurs through the full cross section of the specimen if it is loaded to failure. The assumed elastic behavior is no longer valid. Empirical evidence has shown that the static strength of a notched specimen for moderate K_t-values is of the same order of magnitude as the material tensile strength. It implies that the fatigue limit line for the notched specimen for an increasing mean stress should converge to the point $(0, S_U)$.

For a relatively high mean stress on a notched specimen, the maximum peak stress at the root of a notch will exceed the yield stress. Some plastic deformation occurs and a plastic zone at the notch root is created, see Figure 7.8. The maximum stress would be $K_t S_{\max}$ if plasticity did not occur, but if the peak stress exceeds the yield stress the maximum peak stress is leveled off to a lower value, see S_{peak} in Figure 7.8. After reversion of the load ($S_{\max} \rightarrow S_{\min}$) elastic unloading will occur. Deformations during unloading are elastic deformations. This is the situation sketched in Figure 7.8 where the stress distribution at Smin is also indicated. Although the minimum stress on the specimen is still positive, a compressive stress can occur at the edge of the hole. Full unloading would further increase the compressive stress at the notch. The latter event was discussed in Chapter 4 on residual stresses. The elastic unloading in Figure 7.8 implies that the stress range at the root of the notch is not affected by the plastic deformation. As a result, $S_{a,\text{peak}}$ remains the same, but $S_{m,\text{peak}}$ is reduced by an amount $K_t S_{\max} - S_{\text{peak}}$. The

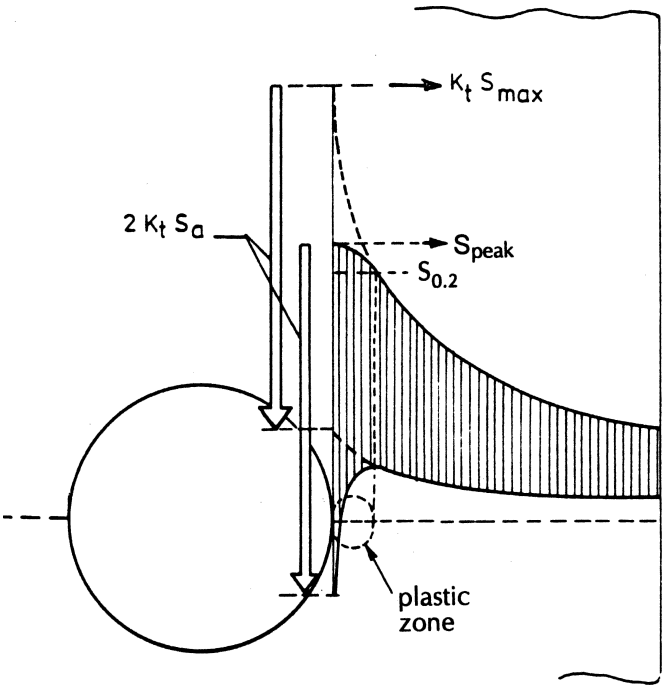

Fig. 7.8 Plastic deformation at $S_{\max}$ in the first cycle, followed by cyclic elastic deformation afterwards. $S_m > 0$.

reduction is advantageous for the fatigue limit S_{fk} although it complicates the prediction of S_{fk} with the similarity principle.

For the onset of root notch plasticity, the yield stress will be used as a criterion. In a notched flat specimen, plasticity at the root of the notch occurs if:

$$K_t S_{\max} = K_t(S_m + S_a) > S_{0.2} \tag{7.15}$$

The boundary line for elastic behavior of the notched specimen is thus given in the fatigue diagram by

$$K_t(S_m + S_a) = S_{0.2} \tag{7.16}$$

This line with an angle of 45° to the axis of the S_a-S_m diagram is drawn in Figure 7.9. The location of the line depends on K_t. For low S_m-values, elastic conditions still exist up to point D in Figure 7.9, and the fatigue limit of the notched element (S_{fk}) is obtained with the method discussed before. However, for a larger mean stress, for instance in point B, the similarity conditions based on point C of the unnotched specimen curve is no longer

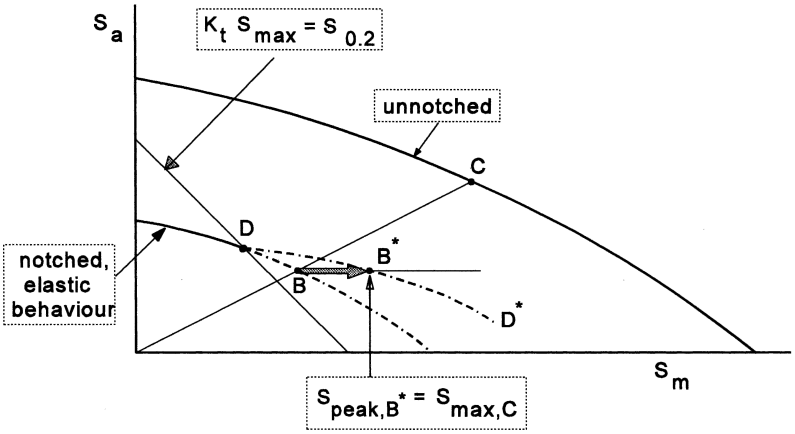

Fig. 7.9 Prediction of fatigue limit of a notched specimen if plastic deformation at the notch root has occurred.

valid due to some plastic deformation at the root of the notch. As long as unloading is still elastic, the amplitude $(S_a)_B$ is still equal to $(S_a)_C/K_t$, but point B shifts to the right because of notch root plasticity. Due to the increased mean stress it shifts horizontally to point B* where S_{peak} is again equal to $S_{\max}$ in point C of the unnotched specimen. The similarity of the stress cycle at the notch root with the stress cycle in the unnotched specimen is then restored. The prediction requires knowledge of the reduces peak stress due to notch plasticity. An estimate can be made by adopting the Neuber postulate discussed in Chapter 4 (Section 4.4). Anyway, after exceeding the yield limit in the root of the notch, the trend is that a further increase of the mean stress will give a smaller reduction of the fatigue limit then suggested with the dotted line DB. At still higher mean stresses on a notched element, plasticity will no longer be a local phenomenon at the root of the notch. Large-scale plasticity will occur, finally through the full net section when S_m is approaching the ultimate tensile strength S_U.

Examples of fatigue diagrams with fatigue limits of unnotched and notched specimens are given in Figures 7.10a and 7.10b for two different materials, a high-strength Al-alloy with a low ductility, and a relatively ductile low-alloy steel with a moderate strength respectively. The results for the unnotched fatigue limit, $S_{f1}(S_m)$, are noticeably different for the two materials. For the Al-alloy, the shape of the curve is approximately similar to the modified Goodman relation (Figure 6.9) whereas for SAE 4130 steel, it agrees much better with the Gerber parabola (Figure 6.9). Some further comments are relevant:

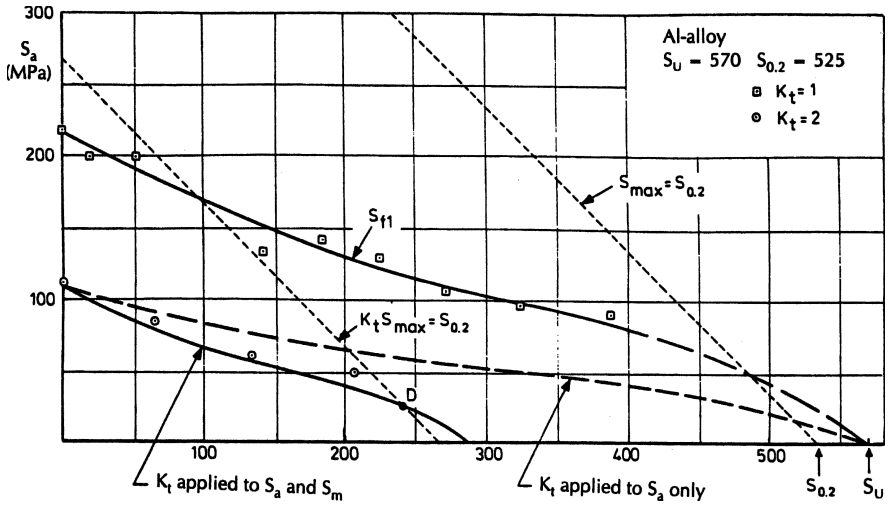

Fig. 7.10 (a) The fatigue limit for $K_t = 1$ and $K_t = 2$ for a high-strength Al-alloy [7, 8].

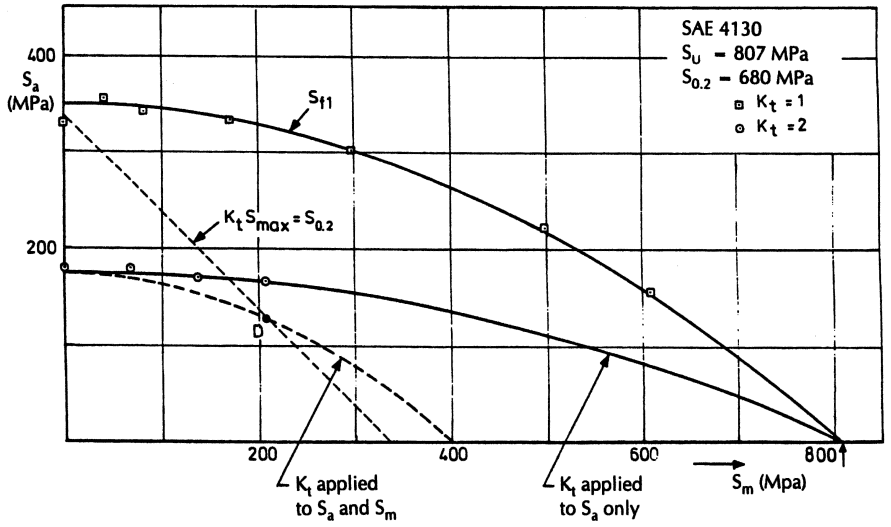

Fig. 7.10 (b) The fatigue limit for $K_t = 1$ and $K_t = 2$ for a low-strength Al-alloy [7, 8].

(i) The mean stress obviously affects the fatigue limit, but the results are not fully systematic. Scatter of the test results around the trend lines can be observed, especially for the Al-alloy.

(ii) If K_t is applied to both S_a and S_m (Equation 7.14), the predicted fatigue limit for the notched Al-alloy specimens agrees reasonably well with the test results. This could be expected because plasticity at the root of the

notch should not occur as long as $K_t S_{\max} < S_{0.2}$). However, the same trend is not observed for the SAE steel 4130. For this material it appears that application of K_t on the stress amplitude only is in good agreement with the experimental data. It may pointed out that this deviation from the simple similarity is a favorable behavior, because the experimental fatigue limits are larger than the theoretically expected values.

The similarity principle is theoretically sound and practically attractive. However, the above results show that the reality does not always follow this simple approach. As discussed in Chapter 6, the fatigue limit of the unnotched material (S_{f1}) can be sensitive to a size effect. In this chapter the size effect was recognized for the prediction of the fatigue limit of notched specimens tested with a zero-mean stress. However, it was not included in the above discussion on the mean stress effect for notched elements. Secondly, the effect of notch root plasticity as sketched in Figure 7.8 is a simplistic model. Notch root plasticity is not exclusively dictated by the yield stress $S_{0.2}$, especially not under cyclic loading. Other methods to estimate Speak at the root of a notch have been suggested in the literature including elasto-plastic finite element calculation. But even then, it is not realistic to expect accurate predictions of S_{fk} as a function of the mean stress. Predictions on the fatigue limit are addressed again in Section 7.7 where comments are made on applications.

7.4 Notch effect under cyclic torsion

The main fatigue loading cases are cyclic tension, cyclic bending and cyclic torsion. Differences between notch and size effects under cyclic tension and cyclic bending are not fundamentally different for predictions of the fatigue limit. However, the situation is different for cyclic torsion. This will be illustrated by two cases:

1. Axles with a stepped diameter or with a circumferential groove, see Figure 7.11. Such geometries are still axisymmetric.
2. Axles with a non-axisymmetric geometry. A simple case is a shaft with a transverse hole, see Figure 7.12.

In the first case, the analysis of the stress distribution is still relatively simple. As shown by Figure 7.11, the K_t-values for torsion are significantly lower than for tension and bending. Also stress gradients perpendicular to the material surface are lower. The semi-empirical methods on predicting notch

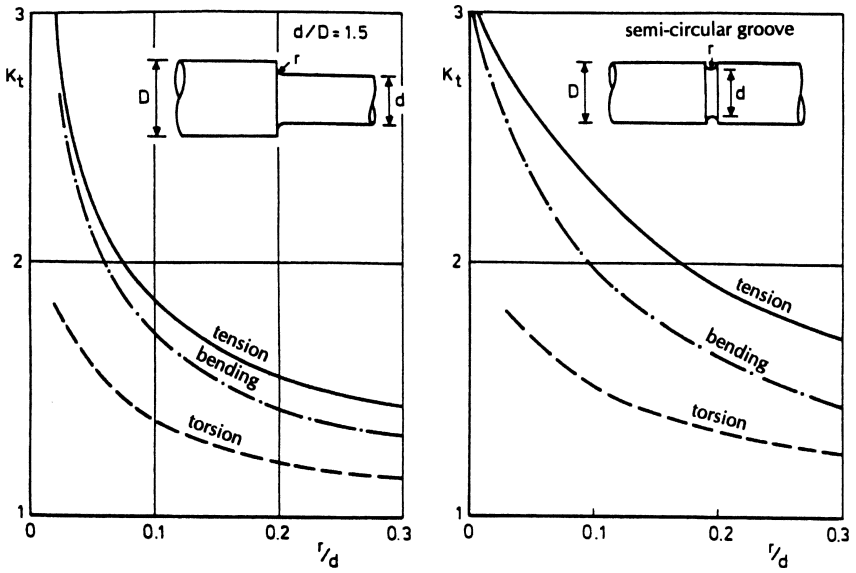

(a) Shaft with shoulder (b) Shaft with circumferential groove

Fig. 7.11 Axisymmetric geometries [1].

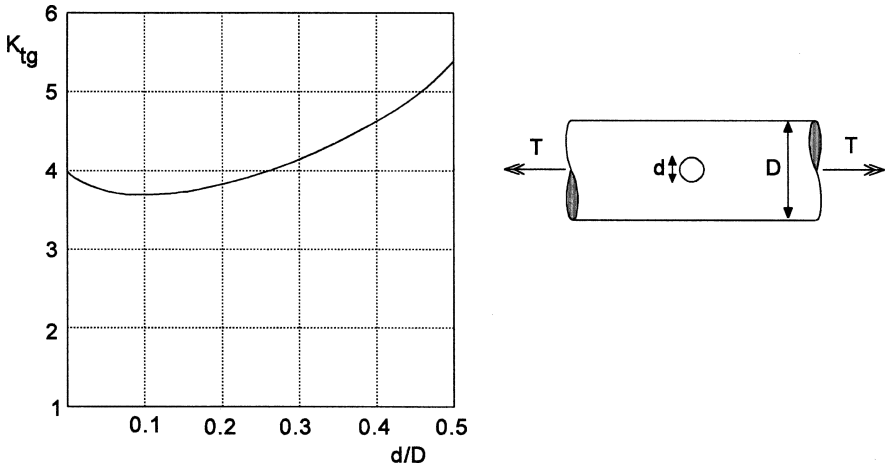

Fig. 7.12 K_{tg} for a shaft with a transverse hole loaded in torsion.

and size effects on the fatigue limit under cyclic tension (Section 7.2) cannot be adopted for this class of cyclic torsion problems because the empirical constants have not yet been obtained and verified. In view of the low stress gradients an obvious approach is to adopt simply $K_f = K_t$, also because K_t-values are relatively low. It should be recalled that the definition of K_t in

this case is:

$$K_t = \frac{\tau_{\text{peak}}}{\tau_{\text{nominal}}} \quad \text{with} \quad \tau_{\text{nominal}} = \frac{T}{\frac{\pi}{16}d^3} \tag{7.17}$$

where T is the torsional moment.

In the second case, the non-axisymmetric geometries, the problem is entirely different. In the simple case of a shaft with a transverse hole, the peak stress occurs at the edge of the hole where a uni-axial tensile stress is present. For that reason, it is more convenient to define the stress concentration factor in relation to the nominally applied shear stress on the gross section:

$$K_{tg} = \frac{S_{\text{peak}}}{\tau_{\text{nominal}}} \quad \text{with} \quad \tau_{\text{nominal}} = \frac{T}{\frac{\pi}{16}d^3} \tag{7.18}$$

For $d \to 0$ the stress concentration factor in Figure 7.12 goes to the classical value: $K_{tg} = 4$ (see Section 3.5, Figure 3.20). In this second case, the notch and size effect as treated in Section 7.2 could again be valid.

Much more complex non-axisymmetric cases are offered by a shaft with a keyseat and a splined shaft, generally loaded under torsion. Peterson [1] offers some K_t data for these cases. But fatigue limit predictions are problematic.

Information on a mean stress effect (τ_m) on the fatigue limit under cyclic torsion of notched specimens is scarce. Because of the small effect of τ_m on the fatigue limit of unnotched specimens under cyclic torsion, it may be expected that the same is true for notched elements with an axisymmetric shape. However, for the second class of geometries (Figure 7.12), a similar mean stress as found for tension and bending should be applicable.

7.5 Notch effect on the fatigue limit for combined loading cases

Combined loading situations can vary from simple cases to rather complex ones. The most simple case occurs in a plate under plane biaxial loading with all cyclic loads occurring in-phase. The biaxial loading can include both tensile loads and shear loads, see Figure 7.13. For an open hole, it implies that the fatigue critical location is on the edge of the hole where a uniaxial stress is present. Stress analysis should indicate the most critical location and the magnitude of the local stress cycle, both amplitude and mean value. For a circular hole, this problem can be solved with equations presented in Chapter 3. Finite element calculation may be required for other types

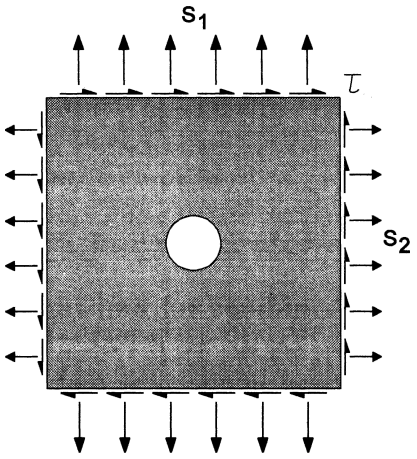

Fig. 7.13 Plate with a hole under biaxial loading.

of holes. The prediction of a fatigue limit then is a problem similar to the problems discussed in Sections 7.2 and 7.3.

The problem is more complex for combined bending and torsion on axisymmetric notch geometries such as shown in Figure 7.11. Assuming again that cyclic bending and torsion occur in-phase, the critical location at the root of the notch is cyclically stressed in a biaxial way. The stress concentration factors for bending and torsion are not the same. Peak stresses at the notch root for bending and torsion are $(K_t)_{\text{bending}} * S$ and $(K_t)_{\text{torsion}} * \tau$ respectively, with S and τ as the nominally applied stresses in the critical section. As discussed in Section 6.3.5, the elliptical quadrant criterion can then be used which should be written here as

$$\frac{(K_{t,\text{bending}}S)^2}{S_{f1}^2} + \frac{(K_{t,\text{torsion}}\tau)^2}{\tau_{f1}^2} = 1 \tag{7.19}$$

It does not include a size effect, but ignoring this effect may be expected to be conservative.

Some other complications must be mentioned. Bending of an axisymmetric specimen induces a bending stress in the direction of the axis of the shaft, but at the same time it also leads to a tangential stress perpendicular to the bending stress, see Figure 7.14. The influence of this smaller stress is unknown from experiments. Usually it is ignored although it could be accounted for by some assumed yield criterion.

A complication is also offered by a shaft loaded under cyclic bending and a constant torsional moment, a situation that can occur in driving shafts.

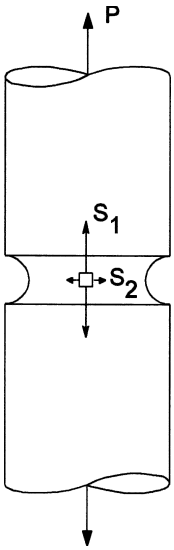

Fig. 7.14 Biaxial stress at the root of a circumferential notch

The question then is whether the constant τ has some influence on crack nucleation. It might be expected that the influence is small and can be disregarded.

Rather complex loading conditions occur when different cyclic loads are out-of-phase and occur with different cyclic frequencies. A crankshaft is an example of such a situation. It is obviously a notched element loaded in bending and torsion in a complex way. The variation of the stress distribution as a function of time can be calculated with finite-element techniques fora fatigue critical location of a structural element. The stress history at the material surface of a notch is still two-dimensional, and it will include both tensile stress and shear stress. In order to arrive at fatigue limit conditions, a sophisticated limit criterion is necessary. A prediction model has been proposed by DangVan [9].

7.6 Significance of the surface finish

As discussed in Section 2.5.5 the surface roughness has a significant effect on fatigue crack nucleation. As a result, the influence on the fatigue limit can be large. In the present chapter, the fatigue limit of notched specimens is discussed in relation to the fatigue limit of unnotched

specimens. The similarity principle used for the predictions starts from the idea that the surface quality is good and similar for both unnotched and notched specimens. In general, unnotched specimens used in the laboratory experiments are manufactured with a high standard of surface quality. The unnotched specimen is provided with a smooth surface finish obtained by fine-turning or even fine-grinding. It should not change the material structure at the surface. A high-quality material surface finish is considered to be essential for acquiring elementary fatigue properties of a material. But it may then be questioned whether a similar surface quality is obtained in an industrial production process of a notched element. A high-quality surface is expensive. Surface qualities are depending on the production technology such as polishing, grinding, turning, contour milling, hole drilling, cutting, sawing, casting, forging, extruding, chemical milling, etc. The effect of different surface finish conditions on the S-N curve and the fatigue limit has been explored in many experimental investigations on specimens of different materials. In many cases this was done for the fatigue limit of unnotched specimens loaded under rotating bending, i.e. with $S_m = 0$. In order to characterize the effect of surface quality, a surface roughness reduction factor γ was introduced. The factor is defined as the ratio of the fatigue limit of unnotched specimens with a specific surface quality and the fatigue limit of the same specimens with a high quality of the surface:

$$\gamma = \frac{S_{1\,f,\text{specific surface quality}}}{S_{1\,f,\text{high-quality surface}}} \tag{7.20}$$

Results from the literature, see Figures 7.15 and 7.16, illustrate how γ can depend on the surface finish and on the static strength of the material. Values significantly below $\gamma = 1$ occur down to 0.5 in Figure 7.15, and to even lower values in Figure 7.16. Both figures show that an increasing strength of steel implies an increasing sensitivity to a poor surface finish. The surface reduction factor γ in Figure 7.15 is characterized by the average roughness depth, R_a in micrometers. Some data on the surface roughness effect for other materials than steel are presented in the literature, but the results are less abundant. Anyway, they show similar trends, i.e. an increasing sensitivity for surface roughness if the strength of a material is increased. This effect is most noteworthy for high-strength Al-alloys.

The question now is whether the same γ values should be applied to predict fatigue limits of notched specimens? Surface roughness implies a superposition of a roughness effect on a geometric notch effect. Regular notches like holes, fillets, etc. have macroscopic dimensions. However, the roughness notches are microscopic notches, but they can be important

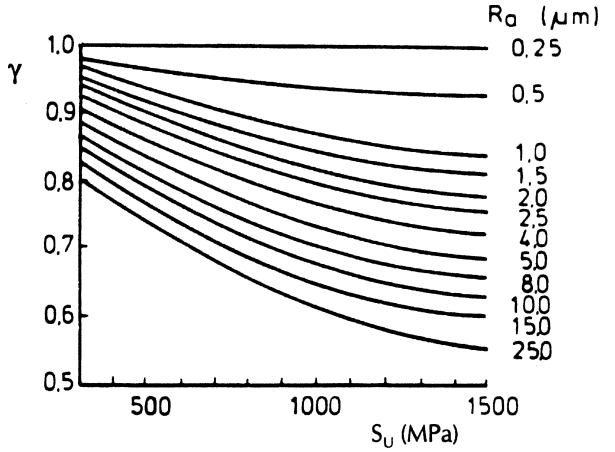

Fig. 7.15 Surface roughness reduction factor γ for steel as a function of R_a (average surface roughness) and the tensile strength (after data in German literature).

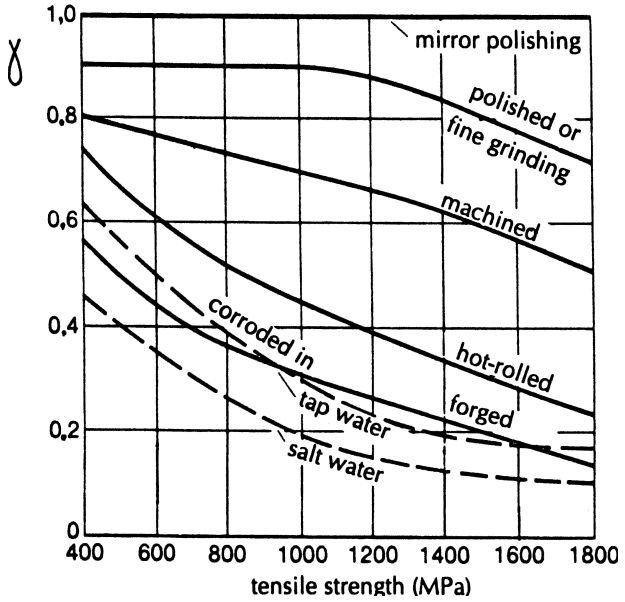

Fig. 7.16 Surface roughness reduction factor γ as a function of the tensile strength of steel [10].

for high-strength materials with a low-ductility. A superposition of notch effects was considered in the discussion on Figure 3.23 (Section 3.6). A multiplication of K_t-values was suggested:

$$K_t = (K_t)_{\text{notch}} * (K_t)_{\text{surface roughness}} \tag{7.21}$$

This is not realistic because the effective root radii of the machining grooves are very small, and K_f should be rather small according to the notch size effect discussed in Section 7.2. On the other hand, it is known from experience in service that surface roughness can substantially reduce the fatigue quality of a structural element of a high-strength material. It is more realistic to apply corrections factors as shown in Figures 7.15 and 7.16 on the predicted fatigue limit to account for the surface quality:

$$S_{fk} = \gamma * (S_{fk})_{\text{predicted}} \tag{7.22}$$

The γ factor as applied in this equation is a reduction factor. The values presented in Figures 7.15 and 7.16 are empirical factors based on results of comparative laboratory experiments. It remains a matter of engineering judgement to decide whether the selected γ-value can be representative for a specific problem. In case of a fatigue critical problem, more accurate information requires that fatigue experiments are carried out on notched specimens. The specimens must be fully relevant for the problem considered, i.e. representative with respect to the notch geometry (especially the root radius) and the surface finish obtained in production.

Two lessons to be learned from the above discussion are:

(i) The advantage of a higher strength material for a fatigue critical element in view of the higher fatigue properties of the material may be offset by the increased sensitivity for the quality of the material surface finish.
(ii) Information on the effect of the surface finishing quality of a product can be estimated (γ-values), but more reliable information requires carefully planned fatigue experiments.

The effect on fatigue of surface treatments, such as nitriding, anodizing, shot peening, etc., is not considered in the present chapter, but comments are presented in Chapter 14.

7.7 Discussion on predictions of the fatigue limit

The fatigue limit is an important material property for many structural elements subjected to large numbers of load cycles. Examples are rotating parts (machinery, engines, etc.) and elements for which vibrations can occur. Large numbers of cycles occur in the service load spectrum of such structural

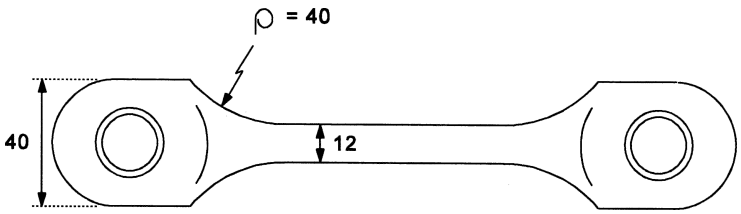

Fig. 7.17 Rod used in prediction example.

elements. In general, fatigue failures will not be acceptable which implies that the amplitudes of all cycles should remain below the fatigue limit. Although safety factors can be applied, as discussed later in Chapter 20, the question remains how accurate the fatigue limit can be predicted in the design stage of a structural element. In the previous sections important variables of the fatigue limit were discussed:

- the stress concentration factor K_t,
- the size of the notch (root radius ρ),
- the surface roughness (quality of surface finish), and
- the type of material.

The effects of these variables on the fatigue limit are understood in a qualitative way. At the same time, this qualitative understanding leads to the conclusion that highly accurate predictions cannot be expected. The question arises if reasonably accurate predictions or conservative predictions are possible. In view of this problem some prediction examples are discussed below.

Prediction examples

1. *Connecting rod,* $S_m = 0$.

A connecting rod of a mechanism as shown in Figure 7.17 should not be heavy in view of fast movements. For that reason, a high-strength low-alloy steel is selected with a tensile strength $S_U = 1000$ MPa. The end fittings are not considered here. They represent a pin-loaded joint (lug) discussed in Chapter 18. However, the cylindrical rod between the end fittings should not fail by fatigue. The maximum tensile load and the maximum compression load are supposed to be equal, and to occur many times. As a consequence, the fatigue limit for $S_m = 0$ is a relevant property to analyse the risk of fatigue failures. If the fatigue limit for unnotched material is not available, it

can be estimated by Equation (6.3):

$$S_{f1} = \alpha S_U$$

Choosing of $\alpha = 0.4$ (to be safe, see Figure 2.12) leads to

$$S_{f1} = 0.4 \times 1000 = 400 \text{ MPa}.$$

A modest stress concentration occurs between the rod and end fittings. The shape of this configuration can be found in the book of Peterson [1], but the ratios of the dimensions in Figure 7.17 are outside the relevant graph in Peterson. However, starting from K_t-values for flat bars and knowing that K_t-values for round bars are lower, it may well be assumed that K_t will be in the order of 1.1 (good design).

Accounting for a notch size effect should not be done. K_f would only be slightly smaller than K_t by a few percent, see Figure 7.4. Moreover, the highly stressed material surface area of the connecting rod is relatively large. A first estimate of the fatigue limit of the critical section is

$$S_{fk}(S_m = 0) = 400/1.1 = 364 \text{ MPa}$$

The following step is to apply a reduction factor γ for the quality of the surface finish. Graphs as shown in Figsures 7.15 and 7.16 should be consulted. The production technique of the connecting rod should give a reasonably good surface finish. The surface roughness could be in the order of $R_a = 5$ μm. The γ-value in Figure 7.15 for $S_U = 1000$ MPa is about 0.75 while Figure 7.16 also suggests that this value could be applicable. Obviously, the choice is somewhat arbitrary. The fatigue limit is now further reduced to

$$S_{fk}(S_m = 0) = 0.75 \times 364 = 273 \text{ MPa}$$

This fatigue limit should now be compared to the maximum load amplitude of the load spectrum of the connecting rod. If the corresponding stress level is indicated by $S_{\text{max,spectrum}}$, it implies a safety margin:

$$\text{safety margin} = 273 \text{ MPa}/S_{\text{max,spectrum}}$$

Whether the safety margin is considered to be sufficient, or too small or too large, depends on a number of questions, such as: Is an occasional fatigue failure acceptable? Is the load spectrum really well known? These questions do not bear upon the accuracy of the fatigue limit prediction. The uncertainties of the prediction of the fatigue limit of the connecting rod

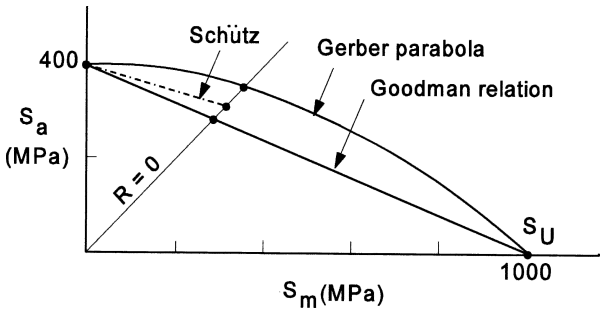

Fig. 7.18 Fatigue diagram for fatigue limit, second prediction example.

are partly a matter of scatter of S_{f1} and the assumptions made (values of α and γ), and for another part due to the variability of the connecting rod as an industrial product. These uncertainties can be accounted for by safety factors, but rational arguments to quantify these factors cannot be offered, other than experience and engineering judgement. If these uncertainties cannot be accepted for economical reasons, it must be advised to do relevant fatigue experiments. The most relevant fatigue tests are tests on the connecting rod itself.

2. *Lifting rod element,* $S_{\min} = 0$, $R = 0$

The rod element has the same geometry as the connecting rod in Figure 7.17. Also the material is the same. The rod is loaded in tension only. Each applied load is followed by an unloading until zero. Because a failure is considered to be fully unacceptable, all applied loads should be below the fatigue limit. In the present case the fatigue limit must be estimated for $S_{\min} = 0$ (or $R = S_{\min}/S_{\max} = 0$). The fatigue limit for unnotched material is again adopted as $S_{f1} = 400$ MPa for $S_m = 0$. But now $S_{\min} = 0$, and a function $S_{f1}(S_m)$ must be adopted. In Figure 7.18, $S_{f1}(S_m = 0) = 400$ MPa and $S_U = 1000$ MPa are used to determine the Goodman relation and the Gerber parabola (Figure 6.9):

$$\text{Goodman relation:} \quad S_{f1} = 400\left[1 - \frac{S_m}{1000}\right]$$

$$\text{Gerber parabola:} \quad S_{f1} = 400\left[1 - \left(\frac{S_m}{1000}\right)^2\right]$$

The line for $R = 0$, i.e. $S_f = S_m$, is indicated in Figure 7.18. The values of S_{f1} for $R = 0$ are found by substituting $S_{f1} = S_m$ in these equations, which

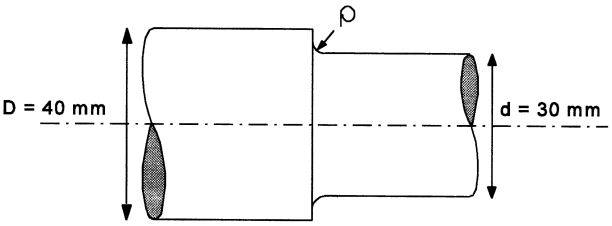

Fig. 7.19 Shaft of the third prediction example.

gives

$$S_{f1} = 286 \text{ MPa (Goodman diagram)}$$

$$S_{f1} = 351 \text{ MPa (Gerber parabola)}$$

These values are substantially different. The S_m-effect as indicated by the data analysis of Schütz, see Figure 6.11, will also be considered. For $S_U = 1000$ MPa, this figure gives $M = \text{tg}\,\alpha = 0.27$. It is easily derived from that figure that

$$S_{f1,R=0} = \frac{S_{f1,S_m=0}}{1+M}$$

Substitution of M gives $S_{f1} = 400/1.27 = 315$ MPa, a value in between the values of the Goodman diagram and the Gerber parabola, but closer to the lower one. Because Figure 7.10b suggests that the Goodman diagram could well be conservative, the result obtained with the Schütz correction is suggested to be an acceptable estimate. The result should still be corrected for the small stress concentration ($K_t = 1.1$) and the same roughness reduction factor of the previous example ($\gamma = 0.75$). It leads to a fatigue limit:

$$S_{fk} = (315/1.1) * 0.75 = 215 \text{ MPa}$$

Because this is an amplitude the corresponding maximum stress for $R = 0$ is 430 MPa, a stress level well below the yield strength of the material.

3. *Rotating bending of a shaft with a shoulder fillet*

Transitions of the shaft diameter in rotating machinery occur for different reasons. An example was shown in Chapter 3 on stress concentrations, see Figure 3.16. The simple geometry to be considered here is given in Figure 7.19. Predictions are made for two steels, a low-strength C-steel ($S_U = 450$ MPa) and a high-strength low-alloy steel ($S_U = 1350$ MPa).

Table 7.1 Predicted fatigue limits.

Material	C-steel		Low-alloy steel	
S_U (MPa)	450		1350	
S_{f1} (MPa)	202.5		540	
$\sqrt{A}$ (mm) (Fig. 7.3)	0.50		0.10	
γ (Fig. 7.15)	0.88		0.72	
ρ (mm)	1	5	1	5
K_t	2.35	1.30	2.35	1.30
K_f	1.90	1.24	2.23	1.29
S_{fk} (MPa)	94	143	175	302

Two root radii (ρ) are considered, viz. a sharp radius ($\rho = 1$ mm) and a generous radius ($\rho = 5$ mm). The results of the analysis are compiled in Table 7.1.

S_{f1} was again estimated with $S_{f1} = \alpha S_U$ with $\alpha = 0.4$ for the high-strength low-alloy steel while a slightly higher value was used for the low-carbon steel, $\alpha = 0.45$. K_t-values are derived from a graph in Peterson's book [1]. The notch size effect was accounted for by the Neuber equation (Equation 7.9), and the surface roughness reduction factor γ was read from Figure 7.15 for a surface roughness characterized by an average groove depth $R_a = 4$ μm (reasonably good finish).

The fatigue limit results S_{fk} on the last line of the table show that increasing the root radius from 1 to 5 mm is beneficial for both materials. The gain is larger for the high-strength low-alloy steel, improvement factor 1.73 compared to 1.52 for the C-steel. This should be expected because of the higher notch fatigue sensitivity of stronger materials, compare K_f-values with K_t-values in the table.

The fatigue limits for the high-strength steel are about two times higher than the fatigue limits for the C-steel, whereas the tensile strength is three times higher. The gain on the fatigue limit is smaller than the gain in static strength. Whether the gain is worthwhile depends on various aspects to be considered by risk analysis and cost-effectivity arguments. In this respect, it is possible that the fatigue limit of the much cheaper C-steel shaft could be improved by some local material surface treatment at the root of the notch, e.g. by rolling (see Chapter 14).

Some general comments on predictions of the fatigue limit

The K_t-value cannot always be derived from data in the literature. In such cases, clever estimates can sometimes be made by considering similar geometries, see also Chapter 3. If accurate values are needed, FE calculations have to be made. The FE techniques are well developed, but care should be taken with mesh-refinements around the notch and with relevant boundary conditions. At the same time, it should be realized that great efforts to obtain accurate K_t-values become less meaningful if other uncertain effects are present and cannot be removed. The effect of the size of the notch (root radius ρ) is accounted for by empirical equations. It cannot be expected that a more rational method with a general validity will be available in the future. The theoretical problem is less serious for high-strength materials because $K_f = K_t$ appears to be realistic. The advantage of $K_f < K_t$ for low-strength materials could be estimated with empirical equations, but the reliability of such equations has certain limitations. The equations were developed primarily for various types of steel whereas the verification for other materials is less abundant, or even non-existent. Under such conditions, predictions on the fatigue limit with the simple methods used in the above examples should be earmarked as "estimates" rather than predictions.

A significant obstacle for predictions on the fatigue limit of notched elements is how to account for the quality of the material surface. It is questionable if this effect can be adequately accounted for by a single surface roughness parameter. True enough, the effect must be considered in predictions, especially because the effect can be large for high-strength materials. In this respect, it should also be recognized that the sensitivity for incidental mechanical surface damage as well as for corrosion damage can be significant (see the lower lines for corrosion damage in Figure 7.16). Designing against fatigue is not simply a question of materials with good fatigue properties. If a material is considered for a dynamically loaded structural element, it should always be tried to collect relevant fatigue data from the literature. With respect to notch and size effects and the significance of the material surface quality, it is also advisable to consult literature data banks with combinations of key words as: name of material, fatigue, notch effect, surface conditions, etc.

As pointed out before, fatigue tests can be desirable if insufficient realistic data are available and if the accuracy of predictions is unsatisfactory. The type of specimen should be as representative as possible for the fatigue problem concerned (notch size, notch shape, surface quality, material, see Chapter 13). With respect to predictions of the fatigue limit, it is noteworthy

that the prediction methodology is historically based on the similarity between fatigue in notched specimens and unnotched specimens. It is an old dream that a fatigue limit for a notched element with e.g. $K_t = 3.0$ should be predictable from the fatigue limit data for the unnotched material, $K_t = 1.0$, which are supposed to be fundamental material data. However, it is more realistic to realize that it is a large extrapolation step to go from data for unnotched specimens with $K_t \approx 1$ to a real structure with geometrical notches with K_t-values in the order of 3.0. If data are available for $K_t = 2.0$ (a value mentioned here as an example), the extrapolation to $K_t = 3.0$ is significantly smaller. A better accuracy could thus be expected, but again due attention must be paid to size effects and surface roughness aspects.

7.8 The S-N curves of notched specimens

The prediction of the fatigue limit of notched elements discussed in previous sections is associated with problems of load spectra with large numbers of cycles while fatigue failures are not acceptable. The fatigue limit then is a most import property. In the present section, predictions of the S-N curve of notched elements are considered. These curves are relevant to problems where crack nucleation cannot be avoided. It then becomes of interest to know how many cycles it will take before failure occurs. A practical question is whether this fatigue life can be accepted as being sufficient for the structure concerned.

As pointed out in the Introduction of this chapter, the prediction of S-N curves is an essentially different problem compared to the prediction of the fatigue limit. The main reason is that S-N data are associated with two different periods of the fatigue life: (i) the crack initiation period including microcrack growth, and (ii) the crack growth period. As discussed in Chapter 2, the transition of the crack initiation period to the crack growth period cannot easily be defined numerically in crack size dimensions. The initiation period is supposed to be completed when microcrack growth is no longer depending on the material surface conditions. The cracks in this period are still microscopically small, and the growth of these cracks can be irregular depending on the type of material and the material structure. The stress intensity factor offers little hope for a reasonable prediction of the crack initiation period.

Another problem about predicting S-N curves is caused by the difference between low-cycle fatigue, say N up to 10^4 and high-cycle fatigue, $N >$

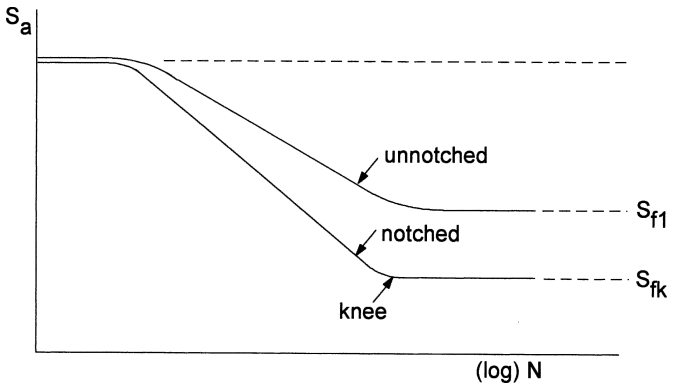

Fig. 7.20 The fatigue strength for notched and unnotched specimens.

10^5 cycles, see Figure 6.3. In the high-cycle fatigue range, the length of the crack initiation period is depending on surface conditions. However, in the low-cycle fatigue range, nucleation will occur immediately due to the high strain amplitudes.

The finite fatigue life in the high-cycle fatigue range of an S-N curve is mainly covered by the crack initiation period. This was discussed in Chapter 6 for unnotched specimens, but is also applies to notched specimens and structural elements with a limited cross sectional area. Visible cracks occur relatively late in the fatigue life. Nevertheless, it is problematic to arrive at some similarity concept for fatigue life predictions. An engineering approach to estimate S-N curves is based on empirical trends observed in relevant test programs. Some characteristic aspects of S-N curves should be recalled here, see Figure 7.20:

(i) As discussed in Chapter 6, S-N curves have two horizontal asymptotes. The lower one corresponds to the fatigue limit ($S_a = S_f$). The upper horizontal asymptote is governed by the static strength: $S_a + S_m = S_U$, see Figure 6.3. The notch effect in a static test is rather small if not negligible. As a result of this relatively small effect, the upper horizontal asymptotes occur at approximately the same stress level for notched and unnotched specimens.

(ii) The location of the knee, i.e. the transition point of the S-N curve to the fatigue limit (Figure 7.20) depends on the type of material, but also on the presence of a notch, the size of the notch and the surface roughness. The knee for unnotched specimens of low-carbon steel is frequently assumed to occur at $N = 2 \times 10^6$ cycles. Al-alloys have a reputation that fatigue failures can still occur at fatigue lives up to 10^7 cycles. However,

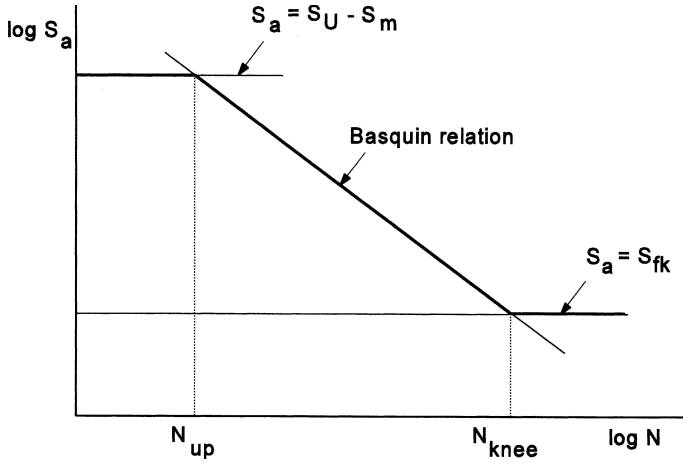

Fig. 7.21 Estimate of S-N curve.

a tendency has been observed that the knee of notched specimens does not shift to high N-values. The knee may occur at a fatigue life of 10^6 to 2×10^6 cycles, and sometimes it can be fairly sharp.

(iii) Between the upper part of the S-N curve and the fatigue limit the Basquin relation ($S_a^k \cdot N = \text{constant}$) is a reasonable approximation, i.e. a linear relation in a $\log(S) - \log(N)$ graph.

With the above observations summarized in Figure 7.21, the following procedure can be adopted for estimating the S-N curve of a notched specimen. First determine the stress levels corresponding to the two horizontal asymptote: $S_a = S_U - S_m$ for the upper asymptote, and $S_a = S_f$ for the fatigue limit asymptote. Secondly, construct a Basquin relationship between the two asymptotes, i.e. a linear relation between S_a and N in a double log plot. The problem then is where this line must be located. The intersections with the two asymptotes are occurring at $N = N_{\text{up}}$ and $N = N_{\text{knee}}$, see Figure 7.21. Considering S-N data of various sources for notched specimens, two conservatively selected values are: $N\text{up} = 10^2$ cycles and $N_{\text{knee}} = 10^6$ cycles.

As an example, S-N estimates will be made for two specimens of SAE 4130 for which S-N curves are available in [8]. The K_t-values of the two specimens shown in Figures 7.22a and 7.22b are 2.16 and 4.0 respectively. The S-N curves are estimated for $S_m = 0$. First the fatigue limit must be predicted which is done with the Neuber equation (Equation 7.9). The material constant $\sqrt{A} = 0.275\ \sqrt{\text{mm}}$ for $S_U = 806$ MPa. With the root radii $\rho = 8.1$ mm and $\rho = 1.45$ mm respectively, and the fatigue limit of the

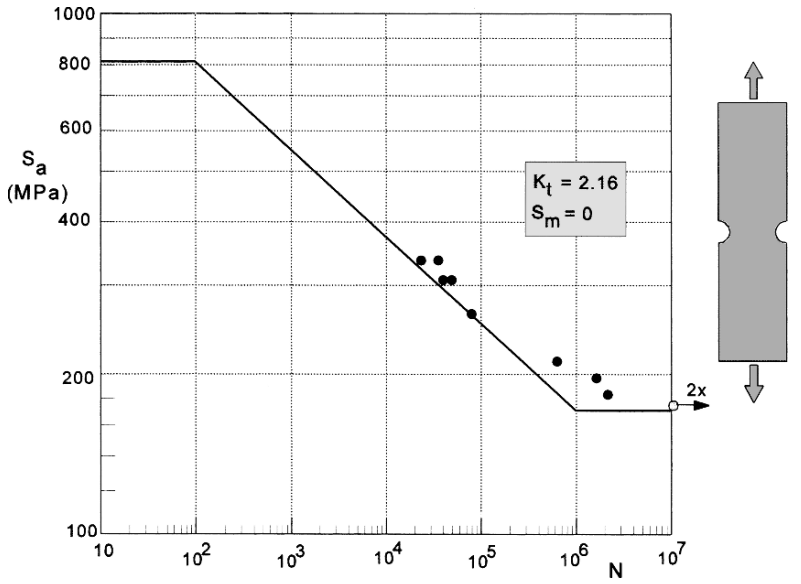

Fig. 7.22 (a) Predicted S-N curve for a mildly notched specimen, root radius $\rho = 8.1$ mm, material SAE 4130 steel.

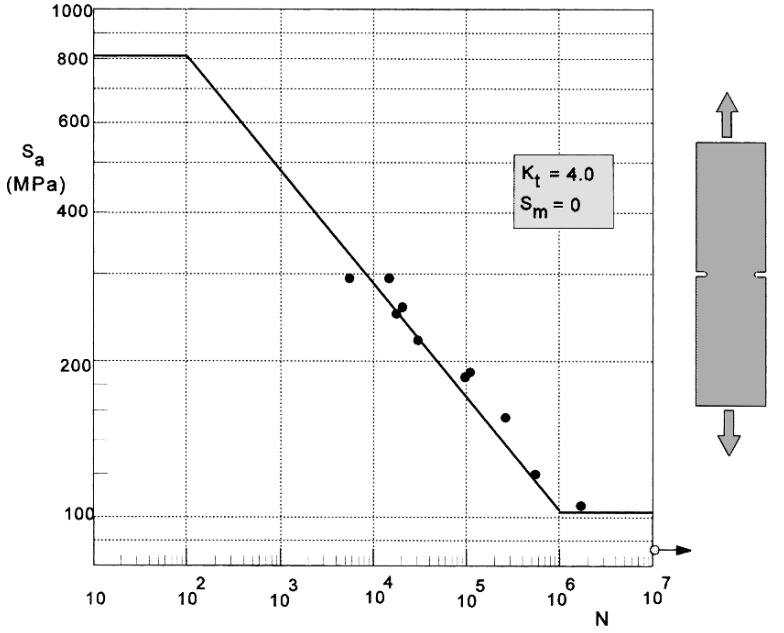

Fig. 7.22 (b) Predicted S-N curve for a sharply notched specimen, root radius $\rho = 1.45$ mm, material SAE 4130 steel.

unnotched material $S_{f1} = 350$ MPa (measured value in [8]), the results are:

$$K_t = 2.16 \rightarrow K_f = 2.06 \rightarrow S_{fk} = 350/2.06 = 170 \text{ MPa}$$
$$K_t = 4.0 \rightarrow K_f = 3.44 \rightarrow S_{fk} = 350/3.44 = 102 \text{ MPa}$$

With $N_{\text{up}} = 10^2$ and $N_{\text{knee}} = 10^6$ the S-N curve can then be drawn, see Figures 7.22a and 7.22b. The experimental results in these figures agree reasonably well with the predicted S-N curves. The calculated slope coefficients k of the Basquin relation ($S_a^k N = \text{constant}$) are equal to 5.9 for the $K_t = 2.16$ specimen and 4.5 for the $K_t = 4.0$ specimen respectively. This order of magnitude is generally observed with a tendency to lower k-values for sharper notches.

It should be recognized that the above empirical approach is in fact an extrapolation from observed trends. Equally good estimates as shown by Figures 7.22a and 7.22b cannot generally be guaranteed. Conservative and non-conservative predictions are possible. The selection of a fairly low N_{up} ($= 10^2$) introduces a slight conservatism. In various cases $N_{\text{up}} = 10^3$ could give better approximations of the S-N curve. The prediction method illustrated by Figure 7.22 is an engineering method which leads to approximate estimates of an S-N curve. Improved predictions require fatigue experiments.

7.9 The major topics of the present chapter

1. *The fatigue limit of notched specimens for $S_m = 0$*
   The fatigue limit depends on K_t (notch effect) and the root radius ρ (size effect). The fatigue limit can be predicted by adopting the similarity principle in its most simple form, which is $K_f = K_t$. The prediction will be conservative in most cases, i.e. $K_f < K_t$. A reasonable prediction of the fatigue limit is possible with empirical equations to account for the notch effect, the size effect, and the strength of the material. The Neuber equation (Equation 7.8) gives reasonable estimates. However, for high-strength materials with a low ductility it is advised to adopt $K_f = K_t$.
2. *The fatigue limit of notched specimens, $S_m > 0$*
   Prediction of the fatigue limit is complicated because local plastic deformation at the root of the notch can level off the peak stress. The mean stress effect can be accounted for by adopting a Gerber parabola for ductile materials with a low or moderate strength level. For

high-strength low-ductility materials, the modified Goodman relation should be advised. In the latter case it is even more safe to apply K_t to both S_a and S_m. Useful indications on the mean stress effect are obtained by the methods of Schütz (Equation 6.5).

3. *The fatigue limit under cyclic torsion*
   For a shaft with a stepped diameter it is advisable to adopt $K_f = K_t$. The mean stress effect should be expected to be small.
4. *The surface finish effect on the fatigue limit of notched elements*
   Predictions on the fatigue limit should include the effect of the surface finish in addition to the notch and the size effect. Reduction factors (γ) of the literature are indicative.
5. *S-N curves of notched specimens*
   Predictions on the fatigue life until final failure are complicated because a finite fatigue life consists of a crack initiation period and a crack growth period. Estimations of S-N curves using the Basquin relation are possible.
6. Important variables for the prediction of the fatigue strength of a notched element are K_t, the size of the notch, surface finish and mean stress. Mechanistic aspects of these variables are reasonably well understood in a qualitative way. Because of this understanding, it is obvious that limitations on the accuracy of fatigue strength predictions should be present. Empirical trends are helpful in making engineering estimates. In fatigue critical cases, experiments are indispensable.

References

1. Peterson, R.E., *Stress Concentration Factors*. John Wiley & Sons, New York (1974).
2. Neuber, H., *Kerbspannungslehre*. Springer, Berlin (1937) (2nd edn., 1958). Translation: *Theory of Notch Stresses*. J.W. Edwards, Ann Arbor, Michigan (1946).
3. Kuhn, P. and Hardrath, H.F., *An engineering method for estimating notch-size effect in fatigue tests of steel*. Report NACA TN 2805 (1952).
4. Siebel, E. and Stieler, M., *Significance of dissimilar stress distributions for cyclic loading*. Zeitschr. VDI, Vol. 97 (1955), pp. 146–148 [in German].
5. Phillips, C.E. and Heywood, R.B., *Size effect in fatigue of plain and notched steel specimens*. Proc. Inst. Mech. Engrs., Vol. 165 (1951), pp. 113–124.
6. Landers, C.B. and Hardrath, H.F., *Results of axial-load fatigue tests on electropolished 2024-T3 and 7075-T6 aluminum-alloy-sheet specimens with central holes*. Report NACA TN 3631 (1956).
7. Grover, H.J., Bishop, S.M. and Jackson, L.R., *Fatigue strengths of aircraft materials. Axial load fatigue tests on notched sheet specimens of 24S-T3 and 75S-T6 alumimum alloys and of SAE 4130 steel*. Report NACA TN 2324 (1951).

8. Grover, H.J., Bishop, S.M. and Jackson, L.R., Fatigue strengths of aircraft materials. Axial load fatigue tests on notched sheet specimens of 24S-T3 and 75S-T6 alumimum alloys and of SAE 4130 steel with stress-concentration factors of 2.0 and 4.0. Report NACA TN 2389 (1951).
9. Dang-Van, K., *Macro-micro approach in high-cycle mutiaxial fatigue. Advances in multiaxial fatigue*. ASTM STP 1191, McDoell, D.L. and Ellis, R. (Eds.) (1993), pp. 120–130.
10. Juvinall, R.C., *Engineering Considerations of Stress, Strain and Strength*. McGraw-Hill, New York (1967).

Some general references

11. *SAE Fatigue Design Handbook*, 3rd edn. AE-22, Society of Automotive Engineers, Warrendale (1997).
12. *Fatigue Data Book: Light Structural Alloys*. ASM International (1995).